SMOKE AND CFD VISUALIZATION OF THE FLOW AFTER AN EMC SCREEN IN A SUBRACK MODEL

R. Antón, M. Castiella, H. Jonsson, B. Moshfegh

SMOKE AND CFD VISUALIZATION OF THE FLOW AFTER AN EMC SCREEN IN A SUBRACK MODEL

Raúl Antón[1, 2, 3], Miguel Castiella[2, 3], Hans Jonsson[1, 2], and Bahram Moshfegh[1]

[1] Division of Energy and Mechanical Engineering
Department of Technology and Built Environment
University of GŠvle, SE-801 76 GŠvle, Sweden

[2] Division of Applied Thermodynamics and Refrigeration
Department of Energy Technology
Royal Institute of Technology, SE-100 44 Stockholm, Sweden

[3] Department of Mechanical Engineering
TECNUN, University of Navarra, Spain

Corresponding email: raul@energy.kth.se

ABSTRACT

An experimental parametric study was performed in order to study the flow pattern inside a radio base station subrack model. The parameters that were analysed are the velocity, the EMC screen porosity and the subrack geometry. The technique used to visualize the flow pattern is the smoke-wire technique.

The objective is not only to gain insight about the influence of those parameters in the flow pattern of the subrack but also to validate the flow pattern predictions of a detailed CFD model. A further objective is to show the importance of using an accurate CFD model in order to visualize the flow pattern in a situation in which there is a 90 degree turn followed by a perforated plate. The fact that the airflow impinges on the screen in an inclined way means that when the flow collides with the interior face of the hole, it suffers a sudden change in direction, even if the perforated plate is very thin. This change in direction is very important in order to get the right flow pattern after the screen.

KEYWORDS: RNG k-ε, perforated plate, porosity, EMC screen, subrack, flow pattern, inclined flow, smoke-wire, flow visualization

1. INTRODUCTION

Enclosing electronics in sealed metal boxes provides good electromagnetic shielding, but evidently restricts the air movement necessary for adequate cooling. In order to meet electromagnetic compatibility requirements, a perforated plate (an EMC screen) must be used. The design of this screen must provide a sufficient free area ratio for the adequate airflow, but at the same time the holes must be small enough to block electromagnetic radiation. According to Ott [1], the maximum aperture size should be less than $1/20^{th}$ of the source wavelength.

Nowadays, thermal management engineers use Computational Fluid Dynamics (CFD) as a design tool to predict the thermal and hydraulic pattern of the airflow at the component level (see Rodgers et al. [2]), as well as at a system level (Lee et al. [3] and Lee & Manhalingam [4]). There are still gaps in system level modelling, such as the uncertainty in input parameters like the screen loss coefficient (Joshi et al. [5]). Many turbulence models have been developed and introduced to the market. It is still required to validate those turbulence models experimentally. Smoke visualization has always had an extended use for visualizations at not high velocity levels. Lohan et al. [6] studied the flow characteristics around a electronic component; among other techniques, they used the smoke-wire method for flow visualization.

Several modelling techniques have been developed and are used at different stages of the design cycle of the product, as is explained by Minichielo and Belady [7]. One possibility is to model several parts in the system level by means of a hydraulic volume or surface resistance as in Nevelsteen [8], where the screens close to axial fans were modelled by a compact model with three directional loss coefficients. Baelmans et al. [9] analyse experimentally the distance of influence by the screen, remarking on the difficulty of predicting the flow beside components placed close to the screen when the screen is modelled by means of hydraulic surface resistance.

In the models that use surface impedance to model the pressure drop, it may not be clear which

pressure loss coefficient to use and which experimental coefficients may be needed. In a typical Radio Base Station (RBS) case, the flow impinges on the screen at different velocities and angles, and it is difficult to choose the proper loss coefficients from the literature. Further, it is not clear which porosity characterizes the model. In most cases the airflow goes through the inlet opening, then makes a 90□ turn (at different velocities) and finally goes through the EMC screen. Quite a lot of complex flow phenomena (such as recirculation) may arise due to the geometry of the subrack. Certainly, the result of modelling the screen could in turn be used to develop correlations for pressure loss coefficients for different geometries.

The objective of this paper is to perform a parametric experiment in order to study the flow pattern inside the subracks of a radio base station model. The parameters that are analysed are the velocity, the screen porosity and the subrack geometry. The technique was used to visualize the flow pattern is the smoke-wire technique. Further, the objective is not only to gain insight into the influence of those parameters in the flow pattern of the subrack but also to compare with the flow pattern of a detailed CFD model of a subrack slot. The detailed CFD model used in this paper has been already validated by the authors in [10], [11] and [12]. In [12], the authors found a good agreement between predicted and observes values of the static pressure drop and local velocities at several locations before and after the screen. But the overall flow pattern was not studied. It is important to use a correct CFD model in order to visualize the flow pattern in a situation in which there is a 90 degree turn and a perforated plate. The fact that the airflow impinges on the screen in an inclined way means that when the flow collides with the interior face of the hole, it suffers a sudden change in direction, even if the perforated plate is very thin. This change in direction is very important in order to get the right flow pattern after the screen. This sudden change in direction is badly predicted if hydraulic surface impedance is used (Anton et. al. [11]).

2. EXPERIMENTAL SET-UP

The experimental validation was performed in a subrack model inside a wind tunnel. The general layout of the wind tunnel is shown in Figure 1.

The wind tunnel walls are made of Plexiglass. The air velocity is controlled by frequency regulation of the electric power driving the fan.

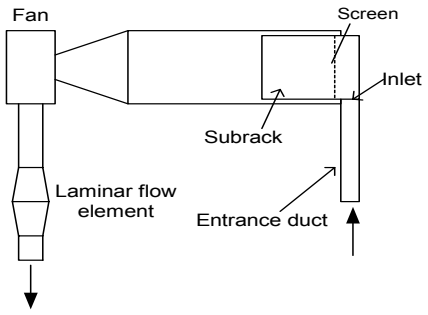

Figure 1. Wind tunnel layout.

A subrack was modelled by means of Plexiglass plates (4 mm thick), as is shown in Figure 2 and Figure 3 (all the dimensions in mm). There are a total of 14 PCB dummies. No heat loads were mounted on the PCB dummies for simplification of the experimental setup and it can be assumed that this will not greatly affect the flow pattern. An entrance duct was placed before the inlet of the subrack in order to get a fully developed turbulent flow at the inlet of the subrack and thus low turbulence intensity levels. Further a perforated plate at the inlet of the entrance duct was used as a turbulence generator in order to decrease the required length needed to create a fully developed turbulent flow at the inlet of the subrack.

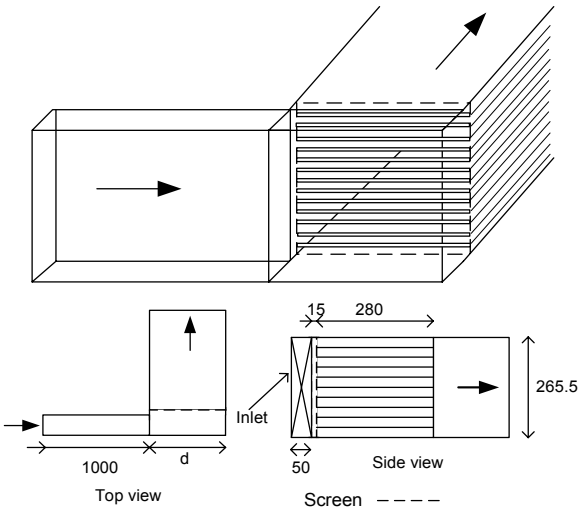

Figure 2. Subrack model.

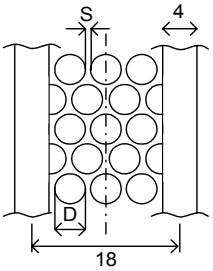

Figure 3. Model of the screen and PCB slot.

Stainless steel screens (1 mm thickness) with 60° staggered circular holes were used. The location of the screen is indicated in Figure 2. Three different porosities, ε, were used for the screen. The porosity in the table below is an approximate value that is calculated using $\varepsilon = n\pi D^2 / 4wd$. Where n is the number of holes in a PCB slot, D is hole diameter, d is the subrack depth (mm) and w is the distance between two PCBs.

Table 1. Screen characteristics (see Figure 3)

	D (mm)	S (mm)	$D+S$ (mm)	ε (%)
Porosity 1	3.75	0.75	4.5	62.2
Porosity 2	3.50	1.00	4.5	54.3
Porosity 3	3.25	1.25	4.5	46.9

Two models were built with the same dimensions except for the depth, d (see Figure 2, top view).

Table 2. Subrack depth for the two models

	Subrack depth, d (mm)
Short case	200
Large case	260

In Table 3 the magnitude of the average inlet velocity is shown for the two models. The average is an approximate value obtained by doing a weighted average from the hot wire measurements along the inlet width of the subrack [10].

Table 3. Average inlet velocities for the two sizes

	Short model (m/s)	Large model (m/s)
V1	1.60	1.65
V2	3.05	3.22
V3	4.43	4.68
V4	5.86	6.14
V5	7.50	7.72

Five wires were placed in the middle between two PCB dummies that are located in the middle of the subrack model. In Figure 4 and Table 4 the distance of the wires from the screen is shown:

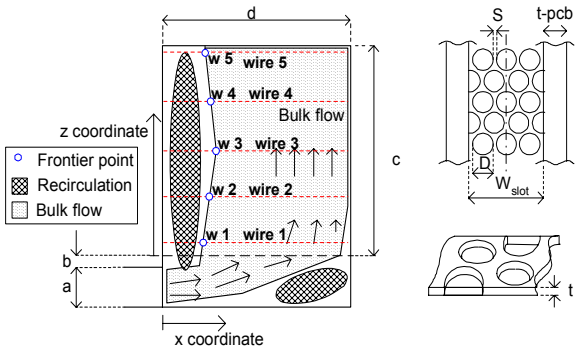

Figure 4. Location of the wires after the screen

Table 4. Distance of the wires after the EMC screen (in mm)

Wire 1	Wire 2	Wire 3	Wire4	Wire 5
16.5	81	146.5	210	276

The smoke-wire technique consists of coating the stretched wires with oil and heating them up. After heating them, the oil evaporates and immediately after that the oil condenses, forming smoke-like micro-droplets. The smoke was illuminated by xenon light. The visualized flow pattern was recorded on video.

The objective of the videos was to identify the frontier line between the bulk flow with a high velocity level and the reversed flow (recirculation) with a low velocity level (see Figure 4). This frontier line is a function of several parameters. Some of those parameters are analysed: the velocity level, the ratio between the inlet and the depth of the subrack, and the screen thickness. The frontier line is identified by 5 points (see w1-w5 in Figure 4). These points are defined for having the z-component of the velocity equal to zero. In order to making it easier to see the frontier point, a black paper was placed on the PCB dummy as in Figure 5.

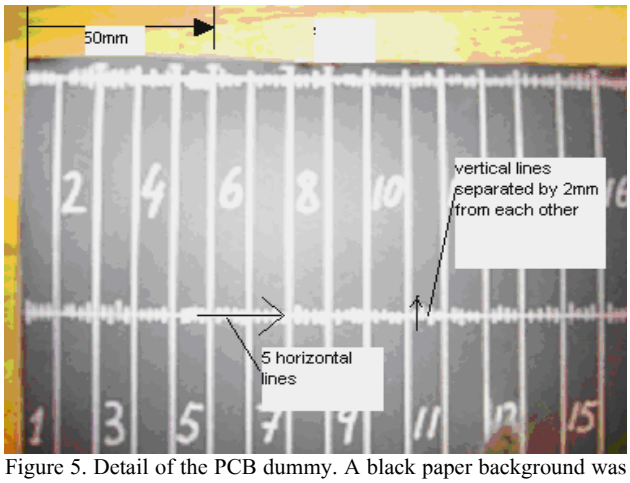

Figure 5. Detail of the PCB dummy. A black paper background was used in order to get a good contrast with the smoke and to distinguish the frontier points.

First it was studied whether the position of the camera influenced the measured frontier points. After 60 videos it was concluded that this factor has small importance due to the fact that the wires are close to the PCB. Actually, the uncertainty of the camera position was estimated to be up to about 0.5 cm (twice the standard deviation of the values observed in the videos).

Furthermore, in order to decrease the uncertainty each wire was recorded between 2 and 5 times.

3. GEOMETRY AND BOUNDARY CONDITIONS OF THE DETAILED CFD MODEL

Due to symmetry conditions, only half of the PCB slot was modelled with the same dimensions as in the experimental model. The dimensions of half of the slot are shown in Figure 6. The flow is considered steady, isothermal and turbulent.

At the inlet of the entrance duct a constant velocity was set and constant turbulence intensity equal to 10%. The result of using constant velocity and turbulence intensity profiles (always 10%) at the entrance duct inlet (see Figure 2) was validated by a comparison between CFD and experimental values of the velocity and turbulence intensity profiles at the inlet of the subrack in a previous paper by the authors [12]. The air density is always equal to 1.2 kg/m^3.

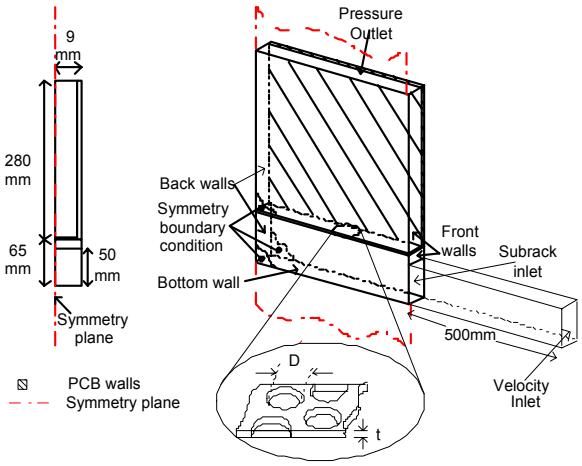

Figure 6. Boundary conditions and geometry of the model (half of the slot between two PCBs is presented).

For the high velocity level (V5), a small pressure gradient was measured at the outlet. However, at the low velocity level (V1) there was no pressure gradient and a constant pressure outlet boundary condition was used. In Table 5, the pressure difference (in Pa) measured and used as a boundary condition in the simulations with the high velocity level is shown. It is necessary to supply boundary conditions for the possible reversed flow at the outlet. Those boundary conditions were always set using a turbulence intensity level equal to 10% and the hydraulic diameter of the outlet.

Table 5 Pressure difference at the outlet and maximum velocity (V5)

Subrack depth (mm)	200	200	200	260
Porosity (%)	46.9	54.3	62.2	62.2
Pressure	1.06	0.915	1.5	1.78

4. MESH DENSITY DISTRIBUTION AND SENSITIVITY

A three-dimensional perforated plate was modelled with circular holes (the holes were done with polygons of 12 sides with an area equal to that of the real hole); the arrangement was 60° staggered and the screen thickness 1 mm (see Figures 2 and 3). The Gambit 2.1 [13] grid generation package was used to generate the mesh. Partial views of the detailed model are shown in Figure 7. The mesh density distribution and sensitivity as well as the overall convergence of the CFD runs were analyze by the authors in [12].

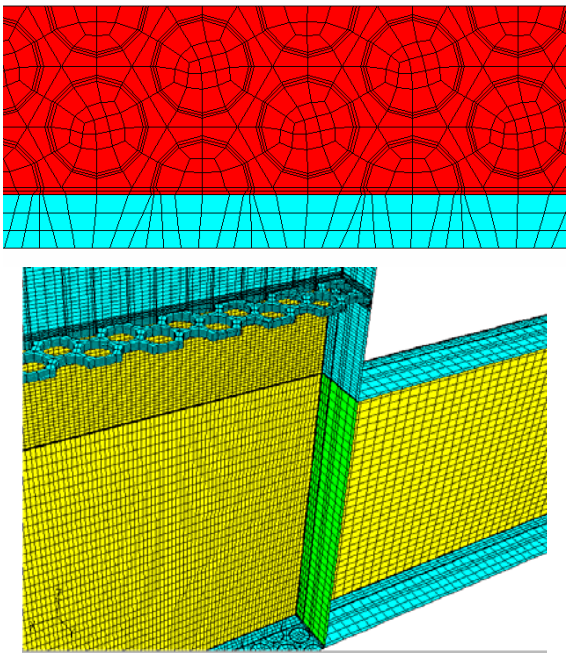

Figure 7. Mesh of the model, partial views.

5. NUMERICAL ACCURACY

FLUENT 6.1 [14] was used for the simulations. The governing equations were solved with a segregated scheme. The momentum, turbulent kinetic energy and turbulent energy dissipation equations were solved with second order upwind schemes. The pressure-velocity-coupling algorithm SIMPLE was used to solve the continuity equation. The following under-relaxation factors were used for the pressure, momentum, turbulent kinetic energy and the dissipation rate of turbulence kinetic energy: 0.3, 0.7, 0.8 and 0.8. The simulation was conducted on a workstation (2.5 GHz). The turbulence model employed was the RNG $k\varepsilon$ model by Yakhot et al. [15]. In [12] an evaluation of the turbulence model was performed, which concluded that the RNG $k\varepsilon$ model was the one that best predicted the pressure drop and the velocity magnitude at several locations.

6. PARAMETRIC STUDY EFFECT OF THE SCREEN POROSITY IN THE FLOW PATTERN

This section is based on the smoke visualizations. In Figure 8, it can be seen how the frontier line moves to the left when the screen porosity decreases, as expected. An interesting aspect is that the smoke visualization gives us qualitative and quantitative information (from the frontier points, see Figure 4). Three cases are shown: a) minimum velocity and short case, b) maximum velocity and short case and c) maximum velocity and large case. In the three cases, it is shown that the bulk flow increases by 2 cm when the screen porosity decreases from porosity 1 to porosity 3 (see also Table 1). Also it is apparent that the ratio between the inlet and the outlet is an important parameter, as it is seen when comparing cases (b) and (c) in Figure 8.

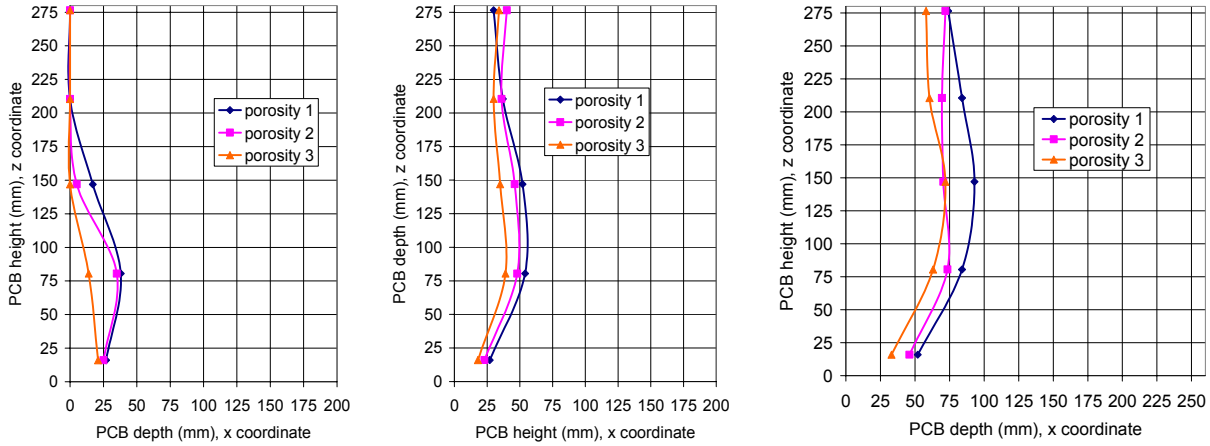

a) Depth = 200 mm, Velocity = 1.60 m/s b) Depth = 200 mm, Velocity = 7.50 m/s c) Depth = 260 mm, Velocity = 7.7 m/s

Figure 8. Effect of the variation of the porosity on the flow pattern based on the smoke visualizations (x and z coordinate in Figure 4).

7. EFFECT OF THE VELOCITY IN THE FLOW PATTERN

This section presents the results from the smoke visualizations. In Figure 9, it can be seen how the frontier line moves to the left when the velocity decreases. There is a large difference between the lowest velocity and the rest of the velocities. Probably the flow for the minimum velocity is in transition, not fully turbulent and that is the reason why the bulk flow (see also Figure 4) is wider at the outlet. The reason why the bulk flow does not distribute across the outlet area is believed to be due to the large inertia of the flow. In the case of the smallest velocity, the inertia forces are not large enough to maintain this uneven distribution and the flow is hence distributed more evenly. The last three velocity levels produce similar frontier lines and thus the velocity has negligible influence on the frontier line.

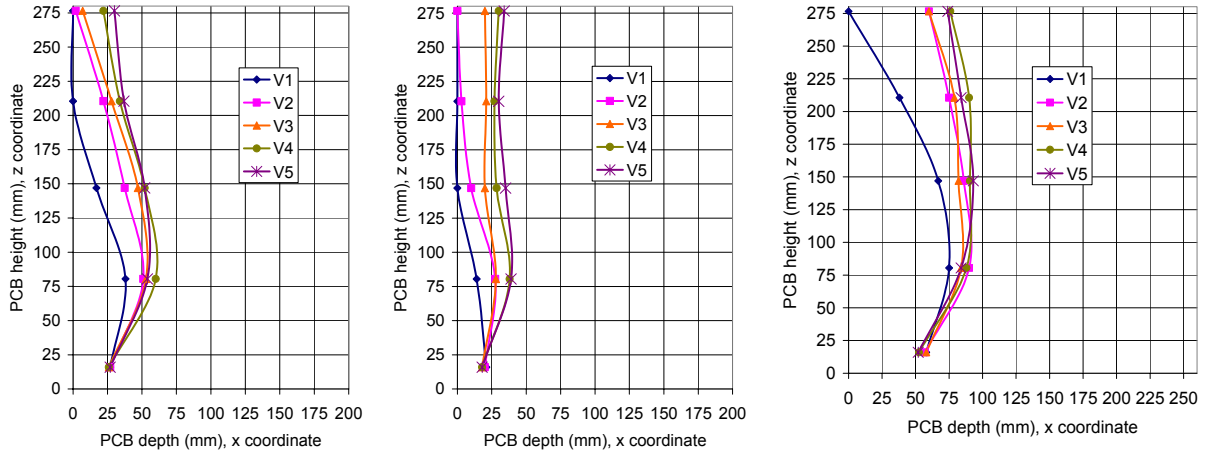

Depth = 200 mm, Porosity 1= 62.2% Depth = 200 mm, Porosity 3= 46.9 % Depth = 260mm, Porosity 1= 62.2%

Figure 9. Effect of the variation of the velocity on the flow pattern, based on the smoke visualizations (x and z coordinate in Figure 4).

8. VALIDATION OF THE FLOW PATTERN PREDICTED BY THE DETAILED CFD MODEL

In the following figures some smoke pictures can been seen of the frontier points for each of the wires and the streak lines that are generated by the smoke. Also, the path lines predicted by the detailed CFD model are shown and the quantitative comparison between the frontier points observed in the smoke visualizations (the average of 5 videos) and the values predicted by CFD. The uncertainty in the observed values is around 0.5 cm (twice the standard deviation of the observed values of the five videos that were recorded per wire), for the wire 5; at the outlet and for the large case, the estimated uncertainty increases up to 0.5-1 cm. In the smoke streak lines and in the CFD path lines, only the first 13.5 cm along the depth of the PCB is shown (see Figure 10).

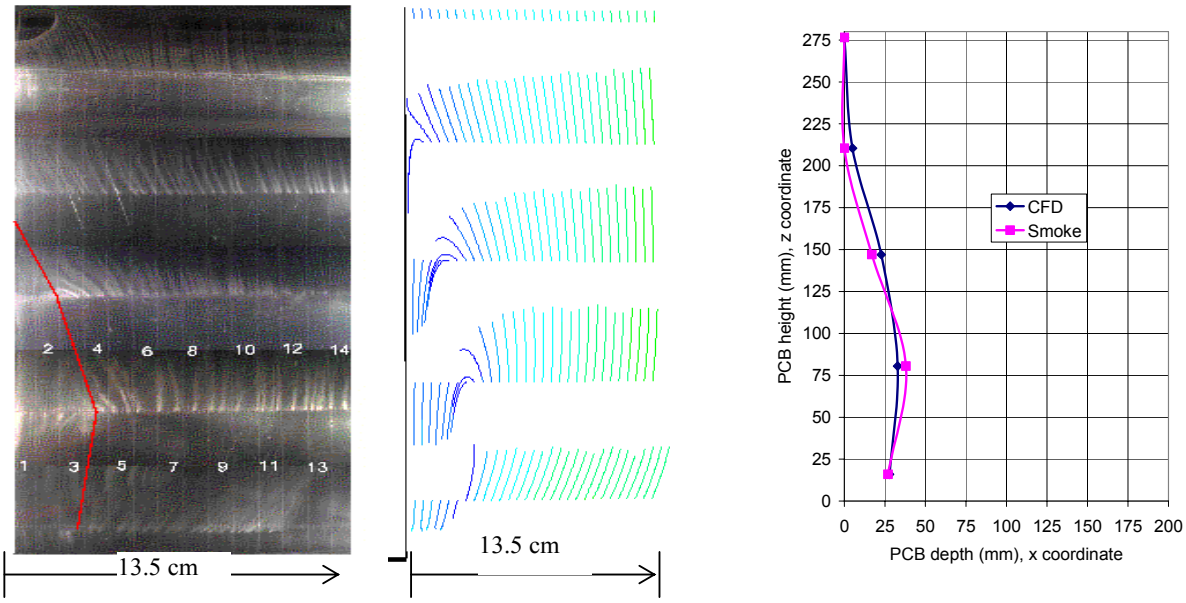

Smoke visualization | Path lines predicted by CFD | CFD vs. Smoke

Figure 10. Validation for the following case: depth=200 mm, V1= 1.60m/s, porosity 1= 62.2%. See x and z coordinate in Figure 4.

In Figure 11 a similar validation for the same case as before is shown, but now at the maximum velocity level (V5).

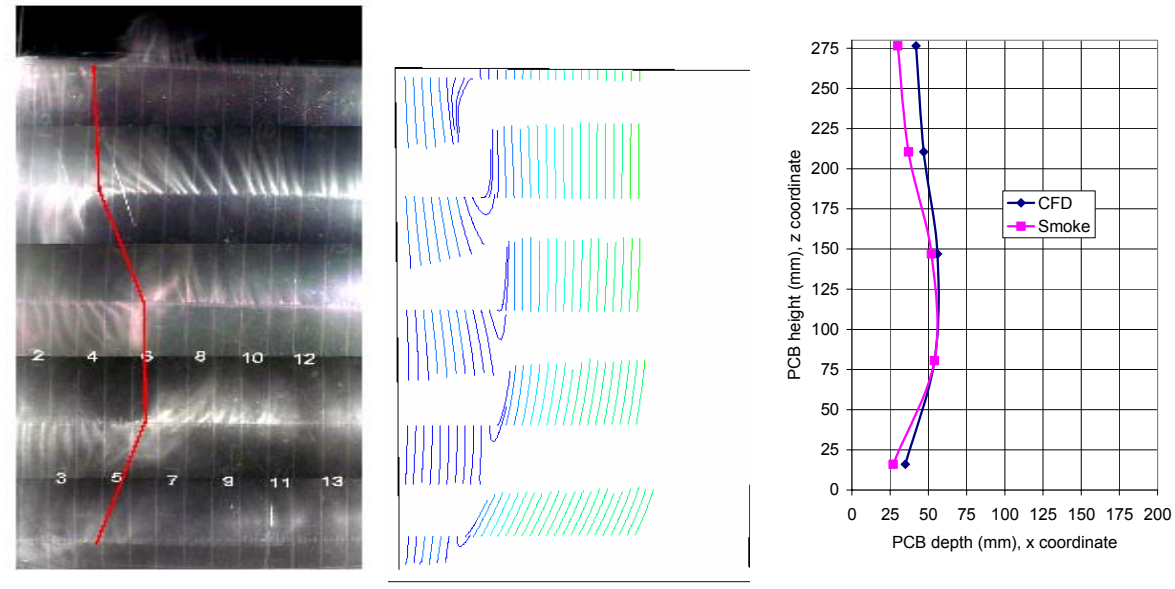

Smoke visualization | Path lines predicted by CFD | CFD vs. Smoke

Figure 11. Validation for the following case: depth = 200 mm, V5 =7.50 m/s, porosity 1= 62.2% (x and z coordinate in Figure 4).

In Figure 12 the same case as before is shown, but now for the minimum porosity (porosity 3)

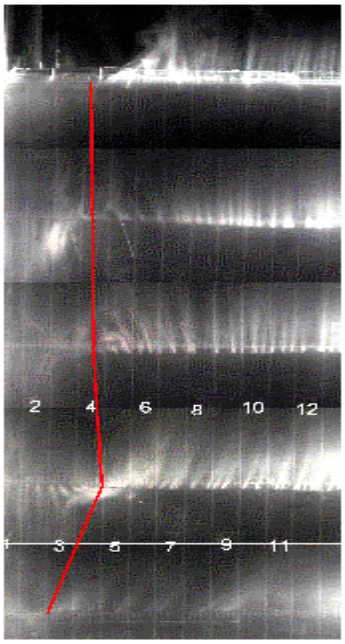

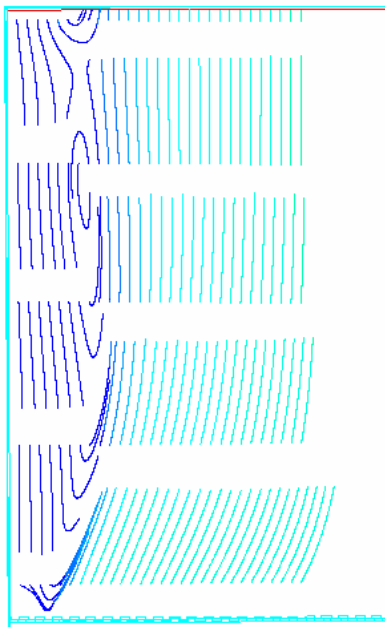

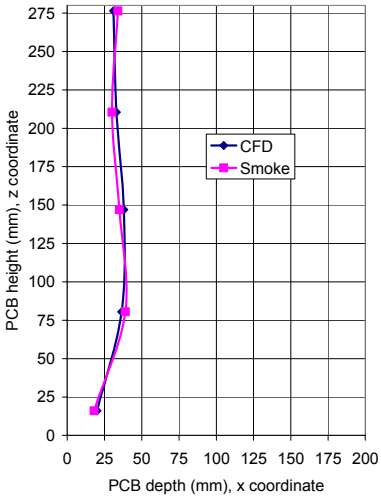

Smoke visualization | Path lines predicted by the CFD model | CFD vs. Smoke

Figure 12. Validation for the following case: depth = 200 mm, V5 =7.50 m/s, porosity 3= 46.9 %. See x and z coordinate in Figure 4.

In Figure 13 shows one case for the large model and a low velocity level (V2). In this case the disagreement between the predicted and observed values is a bit larger. One reason for this is that for the last three wires the flow is quite inclined (not at all perpendicular to the wire around the frontier point) which increases the uncertainty in the smoke visualization.

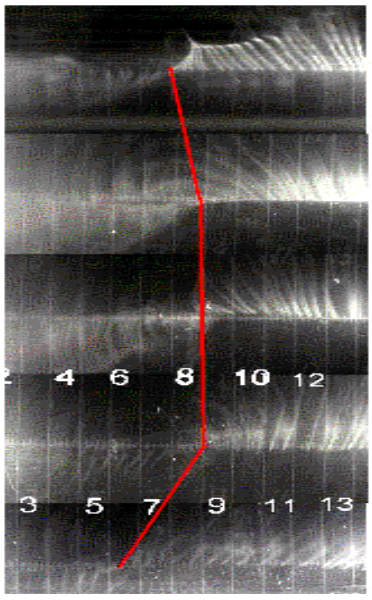

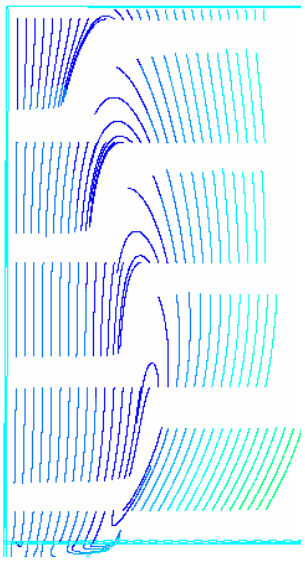

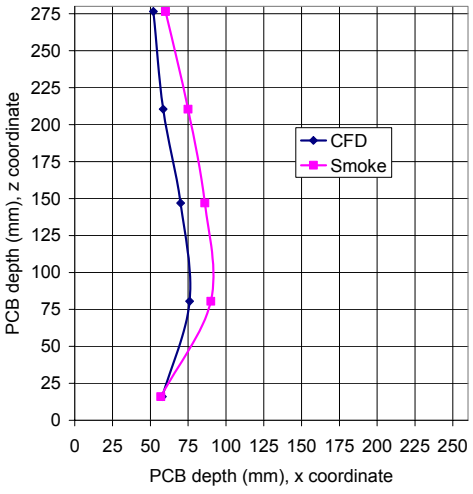

Smoke visualization | Path lines predicted by CFD | CFD vs. Smoke

Figure 13. Validation for the following case: depth = 260 mm, V2 = 3.2 m/s, porosity 1= 62.2%. See x and z coordinate in Figure 4.

It can be concluded from Figures 10 through 13 that the detailed CFD model is able to predict the right change in direction when the inclined flow collides with the interior face of the holes and thus it is a model that could be used to predict how large the bulk flow area is (see Figure 4), which is an important parameter when placing electronic components on a PCB.

9. CONCLUSIONS AND FUTURE WORK

The smokewire technique was applied in a subrack model. The frontier line between the bulk flow (high velocity level) and the reversed flow (low velocity level) has been identified. A parametric study that gives an insight into the flow pattern after the screen was performed with the following parameters: velocity, screen porosity and ratio between inlet and depth of the subrack.

Further, a comparison of the overall flow pattern after the screen for a detailed CFD model was showed. It is apparent that the detailed CFD model has the capacity to predict accurately the flow pattern after the screen. This model will be used in a larger parametric study in which the bulk flow area (or wetted area) will be investigated.

10. ACKNOWLEDGMENTS

The authors gratefully acknowledge the funding received from KK-Foundation, Ericsson, Nokia, Emerson Energy Systems and the Antonio Aranzabal Foundation.

11. REFERENCES

[1] Ott H. W., *Noise Reduction Techniques in Electronics Systems*. Wiley, New York, 1988.

[2] P. J Rodgers., V.C. Eveloy, M.R.D. Davies, "An Experimental Assessment of Numerical Predictive Accuracy for Electronic Component Heat Transfer in Forced Convection Part 1: Experimental Methods and Numerical Modeling" Journal of Electronic Packaging March 2003.

[3] T.T-Y Lee, B. Chambers, M. Mahalingam, "Application of CFD Technology to Electronic Thermal Management" IEEE Transactions on Components, Packaging and Manufacturing Technology, 18(3), August 1995.

[4] T.T-Y Lee and M. Mahalingam, "Application of a CFD Tool for System-Level Thermal Simulation" IEEE Transactions on Components, Packaging and Manufacturing Technology, 17(4), December 1994.

[5] Y. Joshi, D. Baelmans, D. Copeland, C:J.M Lasance, J. Parry, J. Rantala, "Challenges in Thermal Modeling of Electronics at the System Level: Summary of Panel Held at the Therminic 2000" IEEE Transactions on Components and Packaging Technologies, 24(4), December 2001.

[6] J. Lohan, V. Eveloy and P. Rodgers "Visualization of forced air flows over a populated printed circuit board and their impact on convective heat transfer" ITherm 2002. Eighth Intersociety Conference on Thermal and Thermomechanical Phenomena in Electronic Systems, 2002, pp. 501-11

[7] A. Minichiello and C. Belady, "Thermal Design Methodology for Electronic Systems" ITHERM 2002.

[8] K. Nevelsteens et al., "Screen Characterization under Fan Induced Swirl Conditions" 19th IEEE SEMI-THERM Symposium, 2003.

[9] M. Baelmans et al., "Flow Modeling in Air-Cooled Electronic Enclosures" 19th IEEE SEMI-THERM Symposium, 2003.

[10] R. Ant–n, H. Jonsson, B. Moshfegh, "Modelling of EMC Screens for Radio Base Stations Part 1: Experimental Parametric Study" The Ninth Intersociety Conference on Thermal and Thermomechanical Phenomena in Electronic Systems (IEEE Cat. No.04CH37543), Vol. 1, Part 1, 2004, pp. 463-70.

[11] R. Ant–n, H. Jonsson, B. Moshfegh, "Modelling of EMC Screens for Radio Base Stations Part 2: Evaluation of Turbulence Models" The Ninth Intersociety Conference on Thermal and Thermomechanical Phenomena in Electronic Systems (IEEE Cat. No.04CH37543), Vol. 1, Part 1, 2004, pp. 471-8.

[12] R. Ant–n, H. Jonsson, B. Moshfegh, "Detailed CFD Modelling of EMC Screens for Radio Base Stations: a Benchmark Study" Submitted to IEEE Transactions On Components and Packaging Technologies.

[13] *Fluent 6.1*. Fluent Manuals, Fluent Inc., January 2003.

[14] *Gambit 1.2*. Gambit Manuals, Fluent Inc., January 2003.

[15] V. Yakhot , S. A. Orszag, S. Thangam, T. B. Gatski, C. G. Speziale, "Development of Turbulence Models for Shear Flows by a Double Expansion Technique" Physics of Fluids, A 4(7):1510-1520, 1992.